WESC 2025
24 - 27 JUNE | NANTES, FR

Wind Energy Science Conference
24-27 June 2025
Nantes, France

The effect of trailing edge vortex generators on flatback airfoils

Konstantinos Kellaris[a], **George Papadakis**[b], and **Marinos Manolesos**[a]

[a]School of Mechanical Engineering, National Technical University of Athens
[b]School of Naval Architecture & Marine Engineering, National Technical University of Athens
E-mail: kkellaris@mail.ntua.gr

Keywords: Flatback Airfoils, Vortex Generators, Flow Control

1 Introduction

Flatback (FB) airfoils are thick airfoil profiles with a blunt trailing edge (TE) used at the root of modern Wind Turbine (WT) blades, offering several aerodynamic, structural, and aeroelastic advantages [1]. However, although they come with an increase in drag. To counteract this, various drag reduction devices, such as flaps, splitter plates and cavities, have been suggested for FB airfoils [2, 3]. Another common flow control strategy is the use of Vortex Generators (VGs). Typically, VGs are placed on the inner part of wind turbine blades, at a distance of 10% to 30% of the chord length c from the leading edge (LE) on the suction side. They generate streamwise vortices that enhance momentum transfer from the undisturbed flow to the boundary layer developing around the airfoil. This leads to delayed flow separation and, as a result, increased lift. In this work, the streamwise vortices generated by the VGs are used to influence the vortices shed from the thick TE of a FB airfoil. The goal is to suppress vortex shedding near the TE, and as a result to increase base pressure and reduce airfoil drag — a mechanism similar to drag reduction from TE tabs [4].

The LI30-FB10 airfoil [3, 5, 6] is investigated here. The profile has a maximum thickness of $0.3c$ and a trailing edge height of $h_{TE} = 0.106c$, and the investigated Reynolds number is $Re_c = 1.5 \times 10^6$. Triangular VGs with a height of $1.9\%c$ are placed at a streamwise position of $x/c = 90\%$, and arranged at different spanwise distances. Both counter-rotating and co-rotating VG arrangements are examined.

2 Numerical Framework

High-fidelity simulations were performed with the in-house solver MaPFlow [7] to solve the three-dimensional incompressible unsteady Navier-Stokes equations using the artificial compressibility method and the Finite Volume discretization. An O-type mesh extending 50 chord lengths to the far field with approximately 24 million cells was used following previous computational studies [5, 6]. The final mesh 3D was constructed by extruding a 2D mesh along the airfoil span, reaching a spanwise length of one chord discretized with 200 nodes along the span. The maximum non-dimensional distance of the first cell from the airfoil was $y^+ = 0.3$. The simulations were unsteady with a timestep of $dt = 0.002c/U_\infty$ and 70k time steps were performed per case, while turbulence was accounted for using the IDDES method. This hybrid turbulence modelling approach blends the Spalart-Almaras RANS model with the Smagorinsky LES model. Specifically, the RANS variant of the model is employed near the airfoil, while the LES variant is employed away from the airfoil. The necessary grid layers and refinement around the airfoil (RANS region) are shown in Fig. 1(a). Finally, the jBAY model [8] was used to model the effect of VGs using cell distributed body forces. This model is available in MaPFlow and has been extensively validated [9, 10].Fig. 1(b) shows the cells where the jBAY force term is added for one of the examined test cases.

3 Results & Discussion

Firstly, the configuration with no VGs was simulated for two angles of attack (AoA), namely 0° and 12°. The selected AoAs correspond to cases outside and inside the low-drag pocket discussed in [6]. As previously described,

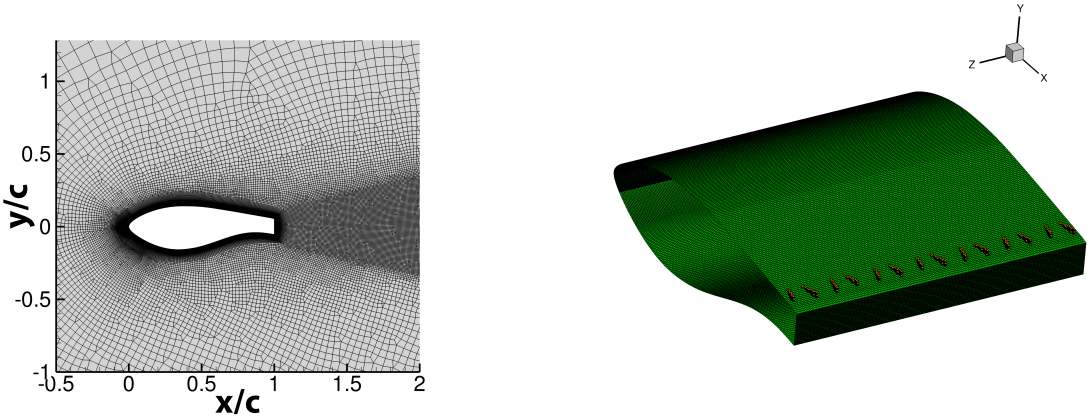

(a) (b)

Figure 1: (a): Detail of the grid refinement layers around the LI30-FB10 airfoil. (b): 3D view of the surface mesh (green). The cells considered by the jBAY model for a VG array of counterrotating pairs that are $L_z = 1.4h_{TE}$ apart along the airfoil span are shown in orange.

VG arrays were placed at the suction side of the airfoil at a streamwise position of $x/c = 90\%$. The VG height h_{VG} is equal to the height of suction side separating boundary layer (BL) $\delta = 1.9\%c$ at 0°. Typical values were selected for the vane angle $\beta = 15°$, the distance between consecutive counterrotating VGs $d = 2.5h_{VG}$ as well as the VG length $s_{VG} = 3h_{VG}$. Different spanwise distances between consecutive VG pairs Λ_z were examined based on the spanwise wavelengths of secondary wake instabilities present in bluff body shedding, namely, $\Lambda_z/h_{TE} = (1, 1.4, 2)$, or equivalently $\Lambda_z/h_{VG} = (5.6, 7.8, 11.2)$. Additionally, a corotating arrangement was examined, where the distance between consecutive VGs was $\Lambda_z = 14.h_{TE}$.

The ratio between the time-averaged Lift coefficient, C_l, over the time-averaged Drag coefficient, C_d, for the different cases is shown in Fig. 2(a). The effect of the VGs is evident, leading to an increase of C_l/C_d compared to the baseline case, that ranges from 5.3% to 17.1% at 0° case and from 0.3% to 3.9% at 12°. Furthermore, the time and space averaged base pressure coefficient is shown in Fig. 2(b).

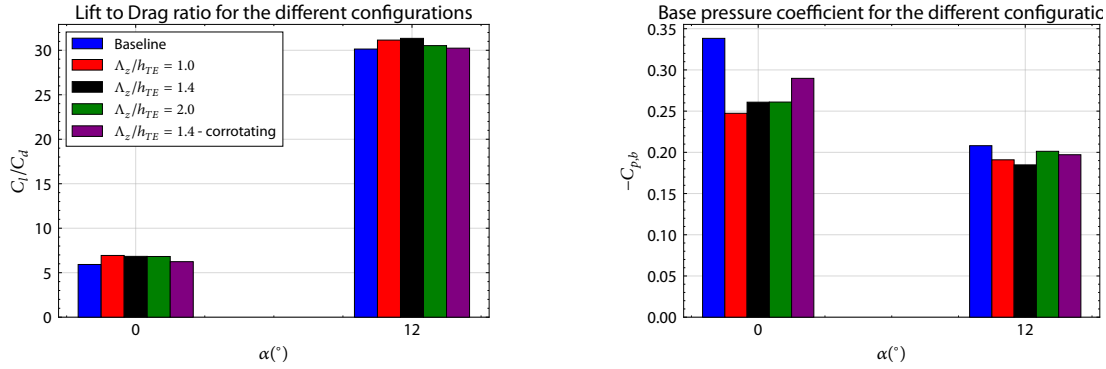

(a) (b)

Figure 2: Performance of the proposed flow control strategy for 4 different configurations: (a): Lift coefficient C_l over Drag coefficient C_d ratio, and (b): Average base pressure coefficient $C_{p,b}$ for the examined cases.

The base pressure recovery, and therefore base drag reduction, is more pronounced at 0°, reaching approximately 26.5% for $\Lambda_z/h_{TE} = 1$. At 12° the maximum increase in base pressure is 11.2% for $\Lambda_z/h_{TE} = 1.4$. Additionally, the cases with the least amount of VGs ($\Lambda_z/h_{TE} = 2$ and $\Lambda_z/h_{TE} = 1.4$-corrotating arrangement) seem to perform the worst, although the case with the most VGs ($\Lambda_z/h_{TE} = 1$) is comparable to the $\Lambda_z/h_{TE} = 1.4$. This leads to the conclusion that the spanwise distribution of the generated vortices and their interaction with the primal and secondary instabilities present in the airfoil wake, also play an important role in the flow control mechanism. This interaction is better illustrated in Fig. 3, where Q-criterion iso-surfaces coloured by spanwise and streamwise vorticity are shown for the baseline and the $\Lambda_z/h_{TE} = 1$ cases at 0°. The suppression of the primary vortex shed

from the suction side is evident for the controlled case compared to the baseline, leading to the enhanced base pressure recovery. Additionally, the generation of streamwise vortices for the controlled case influences the formation of the streamwise vortical pairs connecting successive spanwise vortices (braids) for the baseline case.

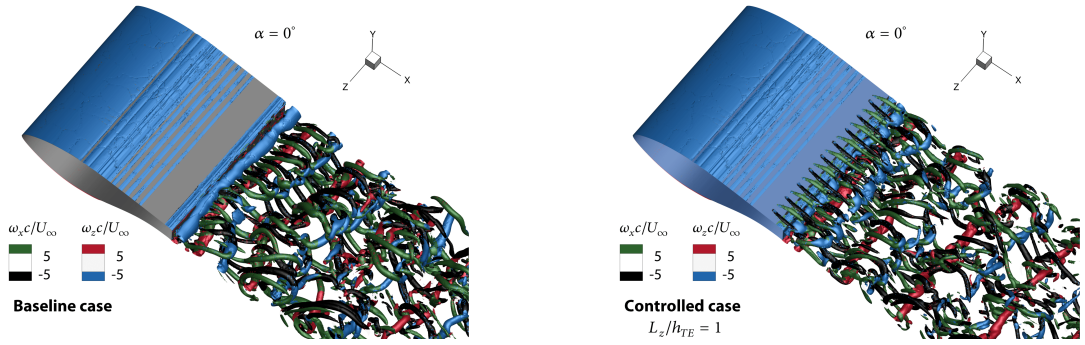

Figure 3: Q-criterion isosurfaces for the $\Lambda_z/h_{TE} = 1$ (left) and the baseline (right) at $\alpha = 0°$. The isosurfaces are colored with non-dimensional streamwise (black and green) and spanwise (blue and red) vorticity.

Acknowledgements

The authors kindly acknowledge the financial support of the European project 'TWEET-IE' funded by the European Union's Horizon 2020 Research and Innovation Programme (Grant Agreement 101079125). K. Kellaris acknowledges the support by the Hellenic Foundation for Research and Innovation (HFRI) under the 5th Call for HFRI PhD Fellowships (Fellowship Number: 20455). This work was supported by computational time granted from the National Infrastructures for Research and Technology S.A. (GRNET S.A.) in the National HPC facility - ARIS - under project "HPC4FAIR" with ID pr014018_thin.

References

[1] J. P. Baker, E. A. Mayda, and C. P. Van Dam, "Experimental analysis of thick blunt trailing-edge wind turbine airfoils," *Journal of Solar Energy Engineering*, vol. 128, pp. 422–431, Nov. 2006.

[2] M. F. Barone, D. E. Berg, W. J. Devenport, and R. A. Burdisso, "Aerodynamic and aeroacoustic tests of a flatback version of the DU97-W-300 airfoil," Tech. Rep. SAND–2009-4185, 1504612, Aug. 2009.

[3] M. Manolesos and S. G. Voutsinas, "Experimental study of drag-reduction devices on a flatback airfoil," *AIAA Journal*, vol. 54, pp. 3382–3396, Nov. 2016.

[4] H. Park, D. Lee, W.-P. Jeon, S. Hahn, J. Kim, J. Kim, J. Choi, and H. Choi, "Drag reduction in flow over a two-dimensional bluff body with a blunt trailing edge using a new passive device," *Journal of Fluid Mechanics*, vol. 563, p. 389, Sept. 2006.

[5] G. Papadakis and M. Manolesos, "The flow past a flatback airfoil with flow control devices: Benchmarking numerical simulations against wind tunnel data," *Wind Energy Science*, vol. 5, pp. 911–927, July 2020.

[6] M. Manolesos and G. Papadakis, "Investigation of the three-dimensional flow past a flatback wind turbine airfoil at high angles of attack," *Physics of Fluids*, vol. 33, p. 085106, Aug. 2021.

[7] G. Papadakis, *Development of a Hybrid Compressible Vortex Particle Method and Application to External Problems Including Helicopter Flows*. PhD thesis, National Technical University of Athens, 2014.

[8] A. Jirasek, "Vortex-generator model and its application to flow control," *Journal of Aircraft*, vol. 42, pp. 1486–1491, Nov. 2005.

[9] M. Manolesos, N. N. Sørensen, N. Troldborg, L. Florentie, G. Papadakis, and S. Voutsinas, "Computing the flow past Vortex Generators: Comparison between RANS Simulations and Experiments," *Journal of Physics: Conference Series*, vol. 753, p. 022014, Sept. 2016.

[10] M. Manolesos, G. Papadakis, and S. G. Voutsinas, "Revisiting the assumptions and implementation details of the BAY model for vortex generator flows," *Renewable Energy*, vol. 146, pp. 1249–1261, Feb. 2020.